



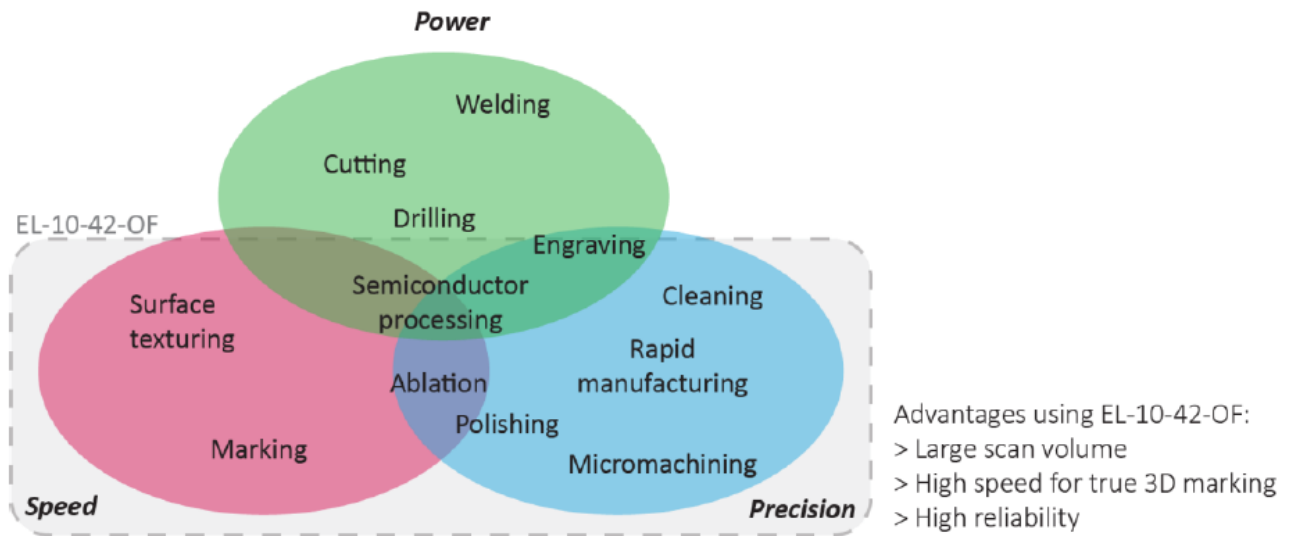
Application note for 2.5D laser processing
using STOT-EL-10-42-OF tunable lens
and
STOT-EL-E-OF-A controller board



1. Introduction

Nowadays, the common solution available on the market for laser processing in 3 dimensions is using the mechanical translation. By moving vertically the marking plane or alternatively by translating a fixed lens with a motor, the z-coordinate can be tuned and controlled. However one major limitation of the former approach is the slow translation speed because it requires massive parts to be moved. The latter allows only a small range in z-travel of about 60 mm for a typical configuration involving an f-theta lens. Owing to the mechanical actuation, the speed by which the spot is shifted is limited. The delicate movable parts are limited in their lifetime, require lots of space to be integrated in an existing system and often need to be water cooled.

In this Application Note, we will describe the integration of the electrically tunable lens STOT-EL-10-42-OF with the controller board STOT-EL-E-OF-A. We will provide general guidelines of using an STOT-EL-10-42-OF lens for the laser marking and engraving application and present a compact 2.5D laser marking system in which the mechanical movement is obsolete. STOT-EL-10-42-OF lens is light, compact and has fast response time (10-millisecond range) as well as long lifetime. Therefore it would be an ideal candidate to overcome many of the downsides of a mechanical solution while at the same time ensuring reduced costs and compact design. STOT-EL-10-42-OF lens is designed for pulsed lasers of near-infrared wavelength between 950 nm and 1100 nm. This opens the possibility to integrate the STOT-EL-10-42-OF into various laser processing applications.



2. Controlling STOT-EL-10-42-OF lens with STOT-EL-E-OF-A controller board

The STOT-EL-E-OF-A controller card is designed to control STOT-EL-10-42-OF lenses. While the STOT-EL-10-42-OF lens shifts the laser spot in z- (vertical) direction, the galvo mirrors deflect the laser spot in the x-y- (horizontal) plane. This approach is implemented in the compact laser marker presented in section 4.3 and schematically shown on the left panel of Figure 1.

The communication between the PC (the user) and the XY2-100 digital controller card is often established via a serial bus, e.g. USB. Within the extended XY2-100 protocol, the z-axis used to control STOT-EL-10-42-OF lens is already available, in addition to the x- and y-axes that control the galvo mirrors. The controller card transmits the digital signal for the x- and y-axis to the scan head for controlling the galvo mirrors. The digital signal of the z-axis has to be converted via a digital-to-analog board (e.g. SCAPS AEB-2 board) into an analog voltage. The right panel of Figure 1 shows another possible integration, in case the XY2-100 controller card has an auxiliary analog voltage output. This voltage output is often used to control an external device such as a z-stage. Both situations do not allow for fast 3D processing since every time the z-coordinate is changed, the machining process is interrupted.

However for many applications where plane objects at different heights are marked, this is a feasible solution. This approach is often referred to as 2.5D laser processing. Only when synchronized via an industrial real-time bus, e.g. the XY2-100 protocol, the key benefit of high focusing speed is fully exploited and enables 3D laser control.

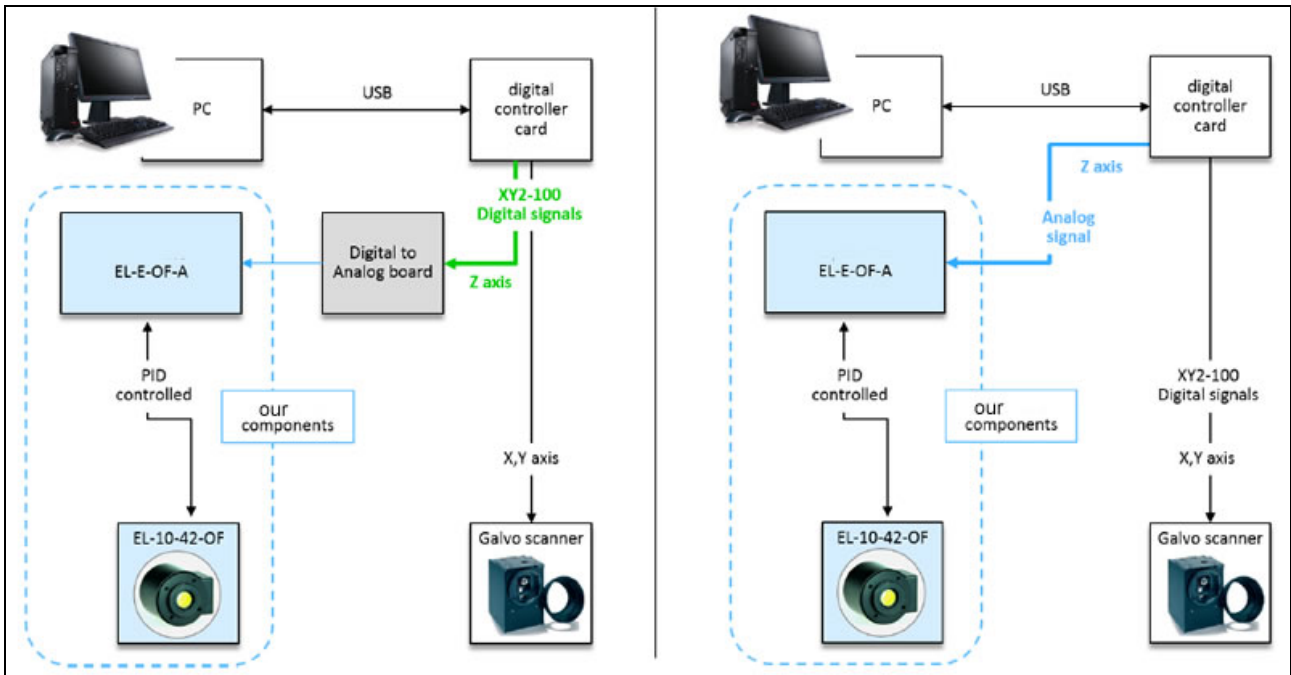


Figure 1: The left panel shows the integration of STOT-EL-10-42-OF within a digital protocol that provides x,y and z-signals. The signal of the z-axis is converted into an analog signal for using STOT-EL-E-OF-A board. On the right, the lens is directly controlled by the analog signal provided by the controller card.

2.1. Calibration of the z-axis

Note that for both cases that are discussed above, or any other possible integration, controlling the lens via the STOT-EL-E-OF-A requires an analog voltage signal ranging from 0 to 5V. The resolution of the signal should be at least 12 bit. The STOT-EL-E-OF-A controls the optical power of the lens and hence allows for shifting the laser spot in z-direction. This is indicated on the left panel of Figure 2.

Two main contributions make it necessary to perform a calibration between the control voltage and the laser spot’s physical z-position in millimetre:

- A nonlinearity in the voltage applied versus optical power characteristics
- Lens to lens variations on the order of 5% to 10% due to production tolerances

After calibration, the set signal directly represents the tuning range in z-direction between Z_{min} and Z_{max} , as shown on the right panel of Figure 2. The actual z-tuning range depends on the precise optical layout in which the STOT-EL-10-42-OF is integrated, see section 4.1. The calibration procedure has to be done once and can be integrated e.g. via a lookup table in the marking software. It is recommended to measure at least five calibration points.

More points will increase the precision of the calibration.

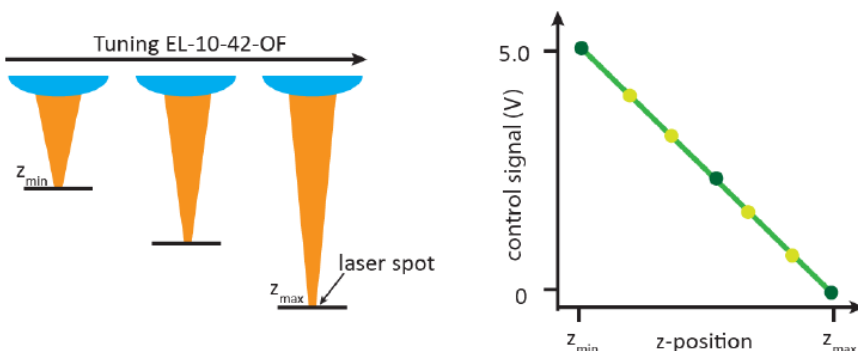


Figure 2: The left panel shows how the z-position of the laser spot is changed by tuning STOT-EL-10-42-OF. The right panel illustrates the calibration curve of control signal (0-5 V) versus the focal

positions in z axis. The light green points represent further points required to increase the precision of the calibration.

3. Response time and oscillation speed

Using the STOT-EL-E-OF-A electronics to control the STOT-EL-10-42-OF, we characterize 3 different situations (step, sinusoidal and triangular signal) that cover most of the “generic” trajectories required in 2.5D laser processing. The results reflect the combined effects of finite bandwidth of the control electronics (dominating part) and the physical limit of the lens itself.

3.1. Step response

The step response of the optical feedback signal itself is measured in order to quantify the speed of focus change. The control voltage at the input of the STOT-EL-E-OF-A is modulated with a rectangular shape at a frequency of 10 Hz. In Figure 4 the blue data show the lower and upper value of the control voltage with 0.5 V and 4.5 V respectively, corresponding to a 10%-90% step. The response of the optical feedback signal is shown in the red data, jumping from -1.6 to +1.6 dpt. In both rising and falling curves, it takes 12 ms to reach the set value within 5% deviation. The small, step-like features of the feedback signal originate from the signal sampling of 1.1 kHz. The data are acquired with an oscilloscope.

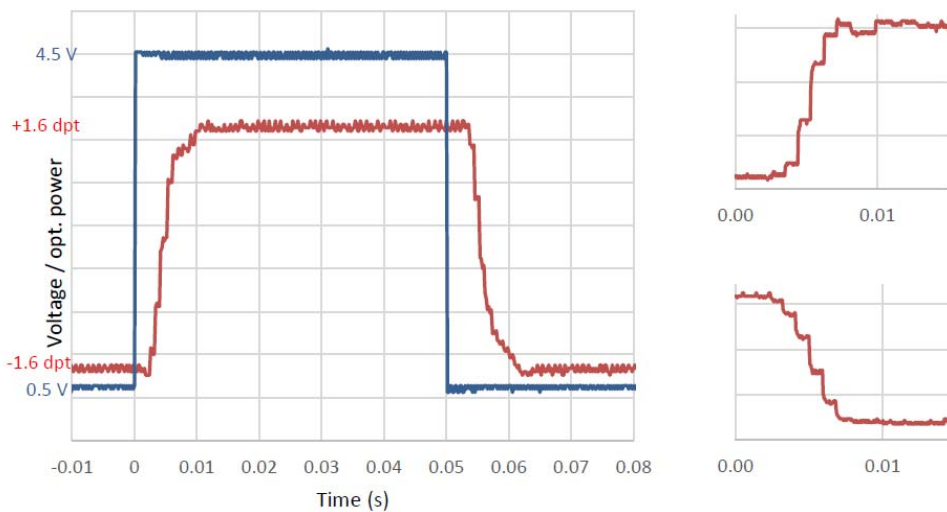


Figure 3: STOT-EL-10-42-OF step response of the optical feedback signal (red). The blue data shows the applied voltage step at the input of the STOT-EL-E-OF-A control board. Both, falling and rising edge show a very similar. The small figures on the left show a zoom on the rising and falling edge. One can see the initial delay of 3.5 ms and the finite rise time of approximately 8.5 ms.

In a more detailed analysis we investigate the scaling of the response time for different step heights. The results are depicted in Figure 4, showing that in general, the total response time decreases with smaller step height. There are two contributions to the total response time. A constant delay of 3.5 ms (dashed line) which originates from the finite sampling rate of the STOT-EL-E-OF-A. And the finite time (finite number of steps) that is required to reach the new set point, typically 6 to 7 steps (blue solid line).

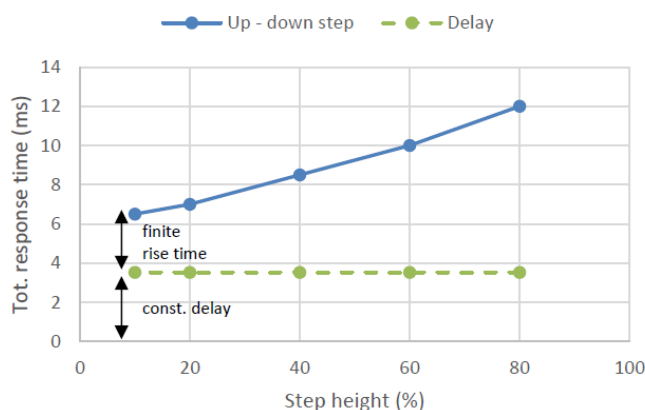


Figure 4: Total response time versus step height. The total response time consists of two contributions, a constant delay and a finite rise time which decreases for smaller step height.

3.2. Sinusoidal modulation

We apply a sinusoidal set voltage with a function generator and observe the amplitude and phase delay of the optical feedback signal. On the left side of Figure 5, the amplitude normalized to the DC limit (constant set voltage) is shown. The amplitude starts to decrease above 40 Hz. The main reason is that there is a constant delay of 5.5 ms, reflected in a linear increase of the relative phase (in degree), shown in the right of Figure 5. When comparing 90% modulation amplitude and 20% amplitude, no significant difference is visible.

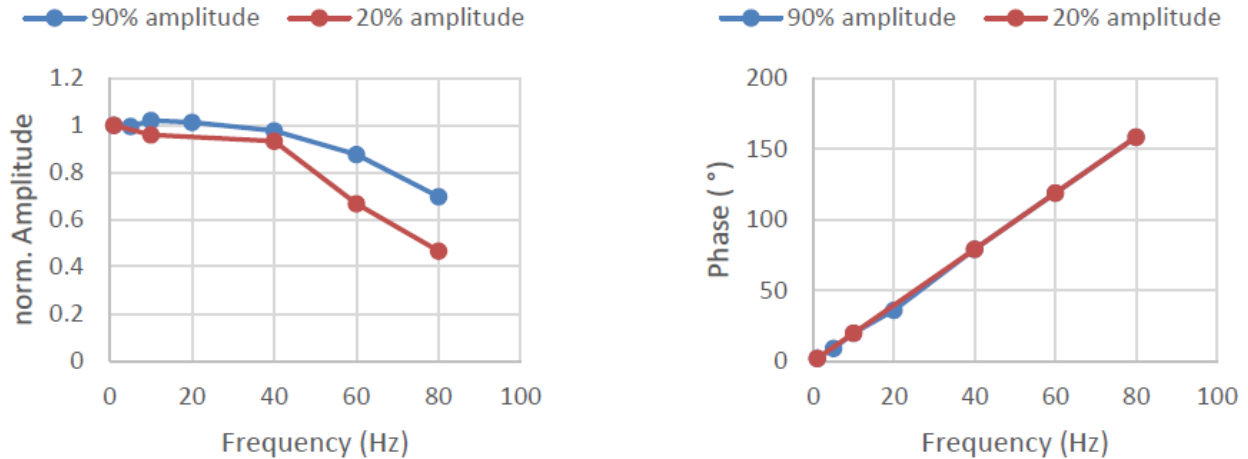


Figure 5: On the left, the normalized amplitude versus frequency is shown. At 40 Hz, the amplitude starts to decrease. Within the measurement precision, the results are equal for the 90% and 20% amplitude. The right side shows the linear increase of relative phase, reflecting a constant delay.

3.3. Triangular modulation

A triangular modulation resembles the processing of inclined planes. Increasing the modulation frequency corresponds to either a steeper plane or increased processing speed. Such a profile is very challenging since even a small delay time leads to a “rounded edge” of the start and end points of the ramps. Consequently, the frequency at which the amplitude starts to decrease is lower than the case of applying sinusoidal modulation. At a frequency of 20 Hz, the amplitude is 90% of the DC limit. Regarding the phase shift, the behavior is very similar to the case of sinusoidal modulation and we observe a constant delay of 5.5 ms.

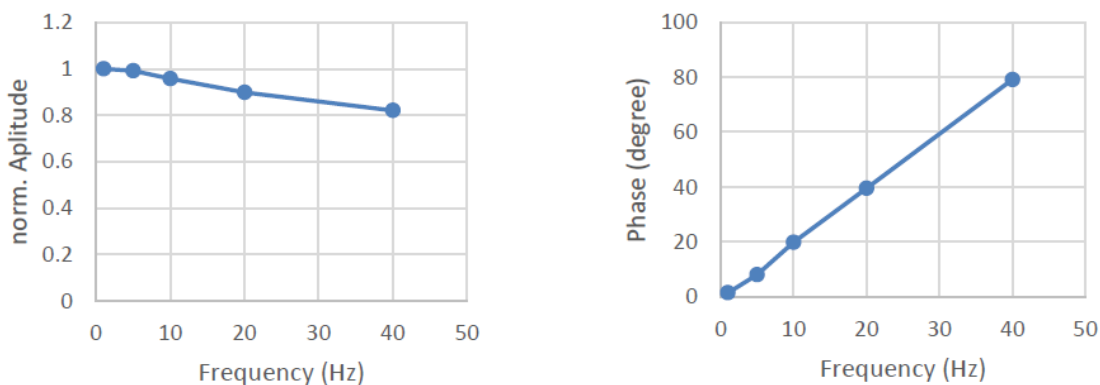


Figure 6: The left side shows the normalized amplitude versus frequency. At 20 Hz, the amplitude is 90% of the DC limit. The linear increase in relative phase, shown on the right side, is characteristic for a constant delay time.

3.4. Conclusion

Compared to 2.5D processing, where the STOT-EL-10-42-OF is used to jump between different z-positions, true 3D processing is more challenging regarding the synchronization of z- and x,y- axis. The main challenge is that the dynamics of the STOT-EL-10-42-OF1(z-axis) is different from the galvo

mirrors (x,y-axis). Most importantly, different delay times, or “acceleration times”, have to be considered by having independent control over z- and x,y- axis at the software end. Higher bandwidth of the control electronics will allow for reaching the physical limit of the lens, which has a resonance frequency of 200 Hz. This indicates that a higher operation speed should be feasible.

4. Optical layout and configuration: with f-theta lens

In Figure 7, the resulting z-tuning range in combination with different f-theta lenses is shown. For larger focal length of the f-theta lens, the resulting z-tuning range as well as the marking field size increases. In each configuration, the focal length of the STOT-EL-10-42-OF is tuned over the maximal range. In general, it is recommended to use the tunable lens before the scanning mirror with a maximal distance of 200 mm between the STOT-EL-10-42-OF and the f-theta lens.

The beam emitted from the laser head has a diameter of about 6 mm. STOT-EL-10-42-OF lens is placed between the laser head and the galvo-scanners. The 6 mm beam diameter does not require additional beam expansion. The beam is reflected by the galvo mirrors that allow beam deflection along x- and y-direction on the processing plane. The field size results from the mirrors deflection angle of +/- 10°. It is not recommended to work at steeper angles due to a reduction of spot quality at the extreme positions. The z-position of the laser spot is changed by tuning the focal length of STOT-EL-10-42-OF lens which enables 2.5D processing, see Figure 7.

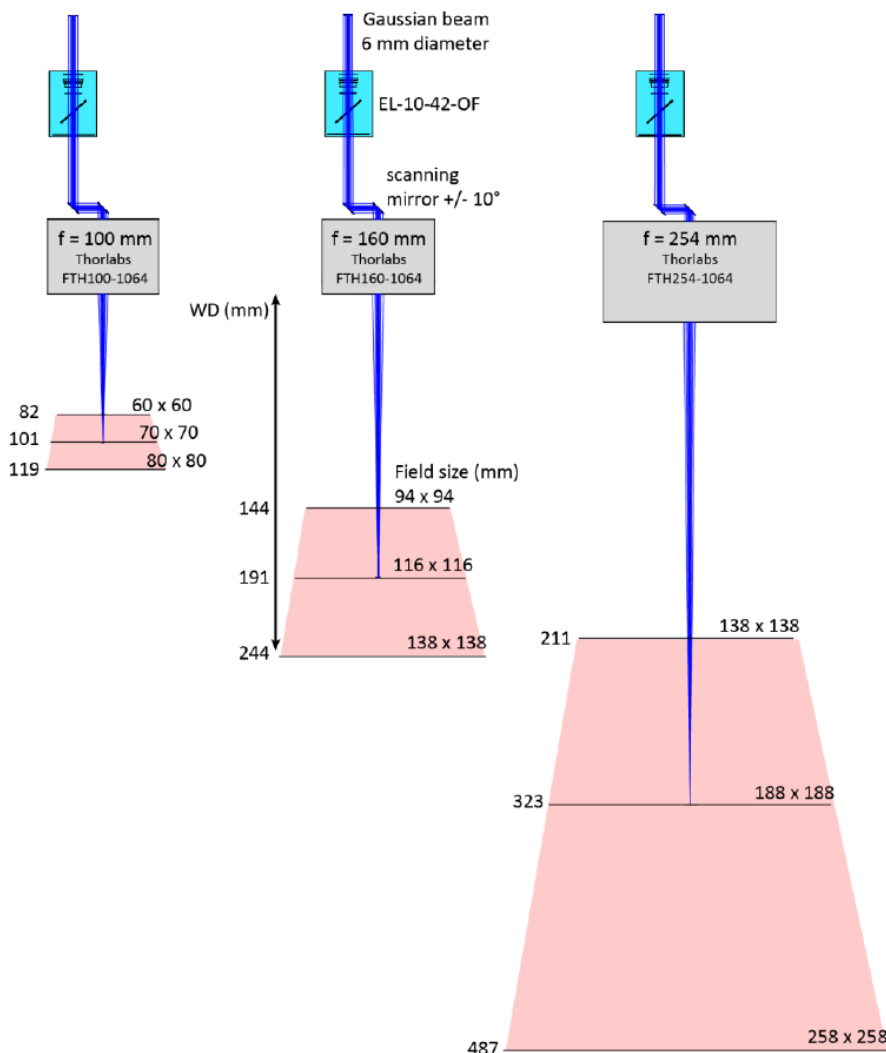


Figure 7: Laser scanning system with the STOT-EL-10-42-OF, galvo scanning mirror and different f-theta lenses $f = 100, 160$ and 254 mm. The corresponding z-scanning range and change of working distance (WD) is indicated by the black arrow. The red color indicates the marking volume for the different situations.

The tunable lens is operated around the zero diopter point with an integrated offset lens that has a focal length of $f_{\text{offset}} = -200$ mm. Field flattening and final focusing onto the marking plane is done by the f-

theta lens. This configuration is very simple to integrate since the STOT-EL-10-42-OF is directly integrated in the existing system. It is especially suitable for situations where the laser spot has to jump between working planes at different heights.

There are remaining field distortions due to imperfections of the f-theta optics. Those effects are slightly enhanced when operating the f-theta lens with the STOT-EL-10-42-OF because of the introduced convergence or divergence of the input beam that enters the f-theta lens. For best marking quality, this has to be taken into account on the software side by e.g. introducing a correction grid.

4.1. Combination with a Galilean telescope

The configurations described in section 4.1 offer a certain degree of freedom regarding the size of working area, z-tuning range and spot size. However, for many applications more flexibility is desirable in order to optimize the tuning range and spot size. This flexibility is enabled by combining the STOT-EL-10-42-OF with a Galilean telescope (beam expander) since it introduces the beam magnification factor as an additional degree of freedom. The generic design is shown in Figure 8. The STOT-EL-10-42-OF is placed between the two fix-focus lenses that constitute the beam expander. The beam at the output is sent onto the scanning mirrors and is then focused by the f-theta lens.

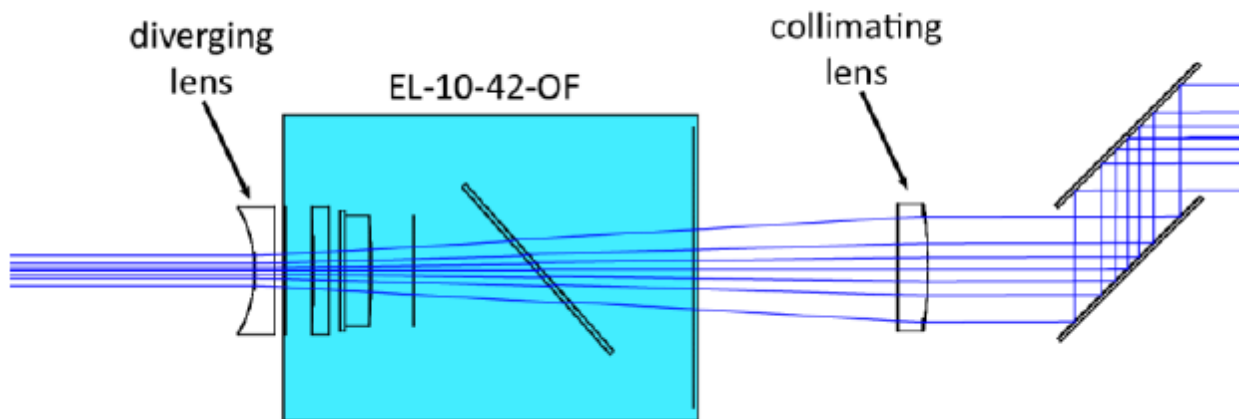
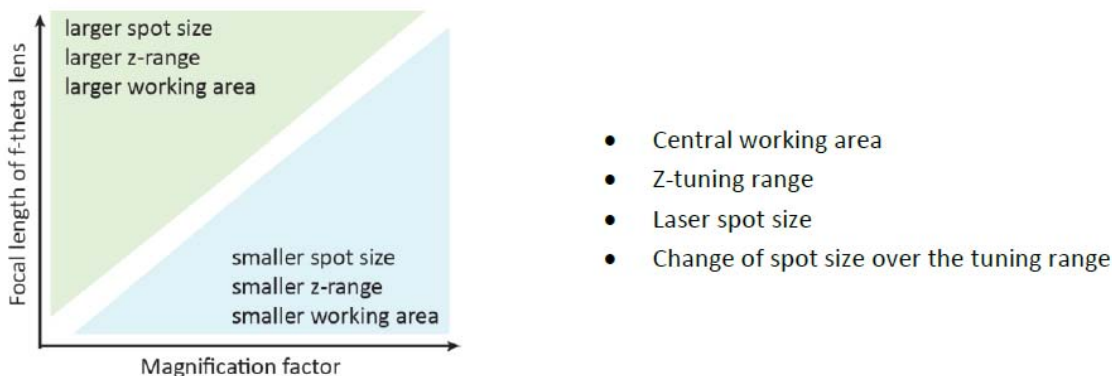


Figure 8: Generic design of a Galilean telescope combined with the STOT-EL-10-42-OF. The beam magnification factor is a crucial parameter to optimize tuning range and laser spot size.


Based on the designs presented in Figure 7, we introduce the Galilean telescope and investigate the scaling of the four most important parameters presented as bullet points below. The graph on the left side already summarizes the qualitative behavior. Note that at a magnification factor = 1 (no beam expander), the results from Figure 7 are recovered, as expected. The color code is consistent throughout the following figures.



4.2. Combination with off-the-shelf beam expanders

As discussed in section 4.1 the spot size and tuning range along the z-axis can be adjusted in combination with a beam expander. Already with off-the-shelf beam expanders a reasonable range of spot sizes and z-ranges are possible. Certain compromises regarding the customization have to be made, however the integration is very simple. The following table presents the different combinations of

expansions factors and f-theta lenses. We verified components from different vendors showing that the results shown in the table negligibly differ by only a few percent.

|  | | 1x | 1.5x | 2x | 3x |
|---|---------------------------|---------------|------|----|----|
| | | (no expander) | | | |
| 100 | Max. input beam size (mm) | 8 | 8 | 6 | 4 |
| | z-range (mm) | 39 | 18 | 10 | 4 |
| | Spot size (um) | 26 | 17 | 18 | 17 |
| 160 | Max. input beam size (mm) | 8 | 8 | 6 | 4 |
| | z-range (mm) | 103 | 46 | 26 | 11 |
| | Spot size (um) | 42 | 28 | 28 | 27 |
| 254 | Max. input beam size (mm) | 8 | 8 | 8 | 6 |
| | z-range (mm) | 263 | 117 | 65 | 27 |
| | Spot size (um) | 70 | 46 | 35 | 28 |

The generic optical setup is illustrated in Figure 9. The beam expander has to be placed as close as possible after the STOT-EL-10-42-OF, however the precise distance is not a very crucial parameter. In order to avoid beam clipping on the galvo mirrors for which the mirror size has to be large enough. Furthermore, the distance between the output of the beam expander and the mirrors needs to be minimized.

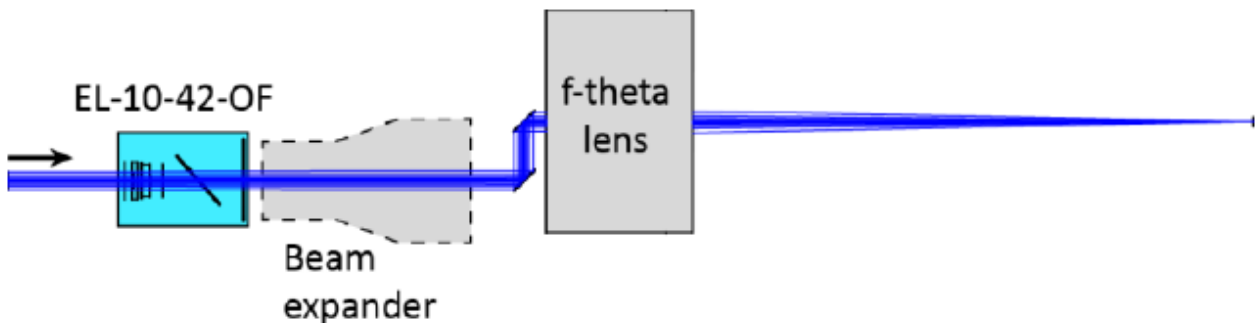


Figure 9: Optical setup to integrate an off-the-shelf beam expander. The beam expander has to be placed directly after the STOT-EL-10-42-OF.

4.3. Integration example of a laser marking system

Figure 10 shows a photograph of a compact laser marking system. This is built for demo. The STOT-EL-10-42-OF is compact enough that it is integrated in the empty space between laser and galvo head (see Figure 11). With this setup, the possible z-travel is enlarged to about twice the range (100 mm) compared to the standard approach. The XY2-100 communication protocol, a widely used industry standard, together with the STOT-EL-E-OF-A controller board guarantees synchronized tuning of the z-position of the laser spot with the galvo scanner unit.



Figure 10: Laser marking system using electrically focus tunable lens STOT-EL-10-42-OF for fast z-axis focusing.

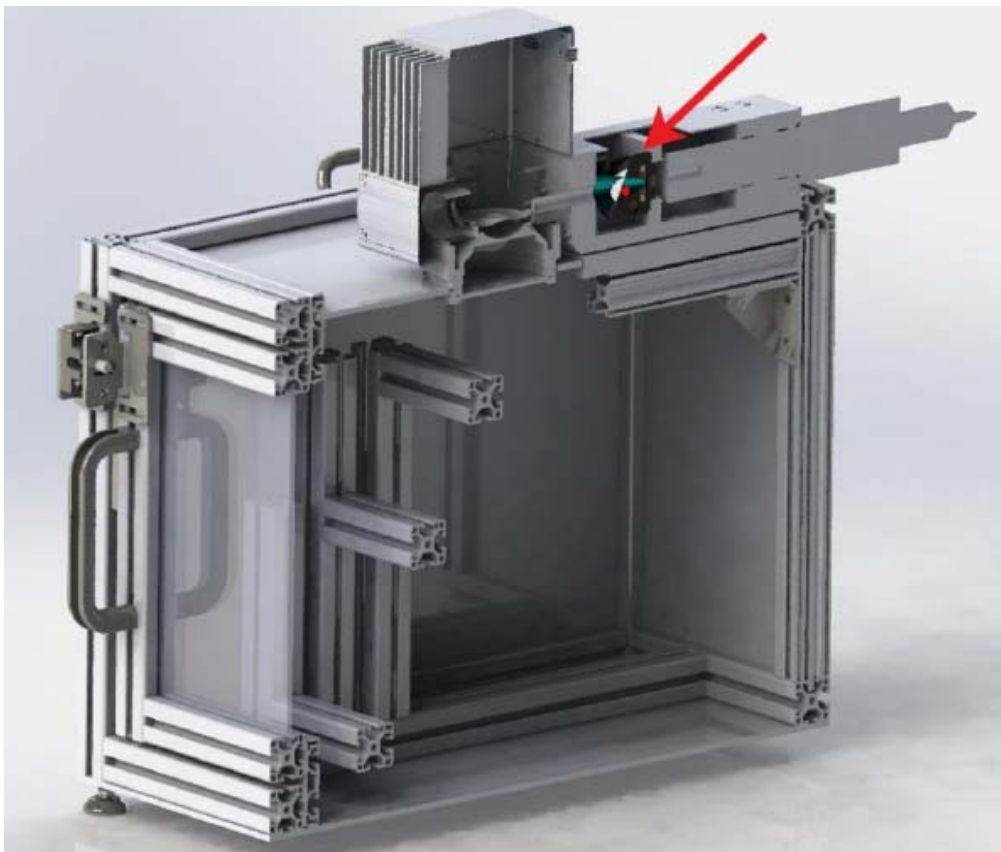


Figure 11: Schematics of laser marking demo setup. The electrically focus tunable lens STOT-EL-10-42-OF is placed between laser head and galvo mirrors, indicated by the arrow.

The following table summarizes the main specifications of the marking system.

| | | |
|---|------------------|------|
| Outer measures | 400 x 400 x 300 | mm |
| Weight | approximately 15 | kg |
| Marking field at central position | 100 x 100 | mm |
| Laser class | 1 (with housing) | |
| Laser vendor | IPG | |
| Maximal laser power | 20 | W |
| Laser wavelength | 1064 | nm |
| Typical spot size | approximately 70 | µm |
| Beam quality M ² (IPG specs) | < 2 | |
| Focal length f-theta lens | 160 | mm |
| Typ. Jump speed | 6000 | mm/s |
| Z-tuning range | 100 | mm |
| Software | SCAPS SAMLight | |

4.4. Marking results

A more detailed view at the obtained marking quality is shown in Figure 12. A 10 x 10 mm rectangle is marked at the two extreme positions of the marking volume. Examining the result under a microscope with 8x magnification, no significant difference or degradation is visible.

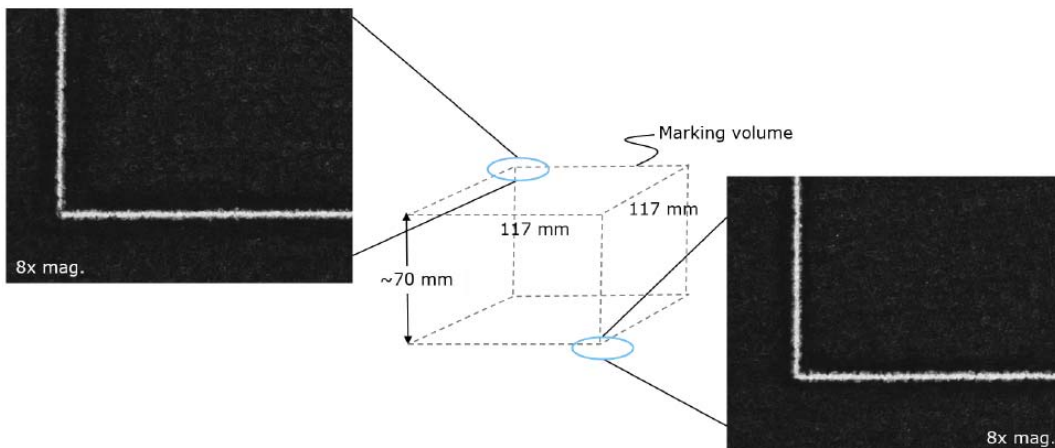


Figure 12: Marking quality at two extreme positions of the marking volume. In both cases, a small 10 x 10 mm rectangle is marked and the result is examined with an 8x microscope. No significant difference is visible.

In a second experiment, we investigate the influence of the STOT-EL-10-42-OF on the marking quality. A dot matrix of 4 x 4 points is marked on a horizontal plane. The left image of Figure 13 shows the result when the STOT-EL-10-42-OF is in the beam path and the right image presents the situation when the STOT-EL-10-42-OF is taken out of the system. Again, the marked samples are investigated with an 8x microscope. As a result, there is no visible degradation due to the STOT-EL-10-42-OF.

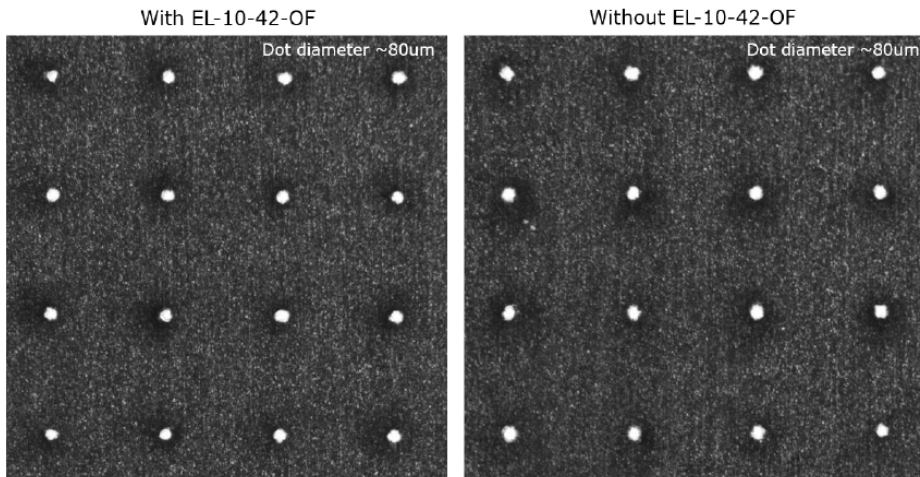
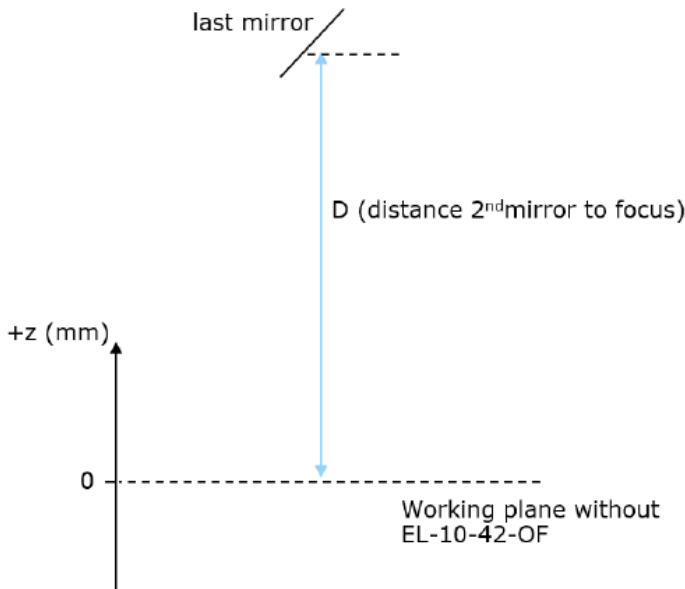


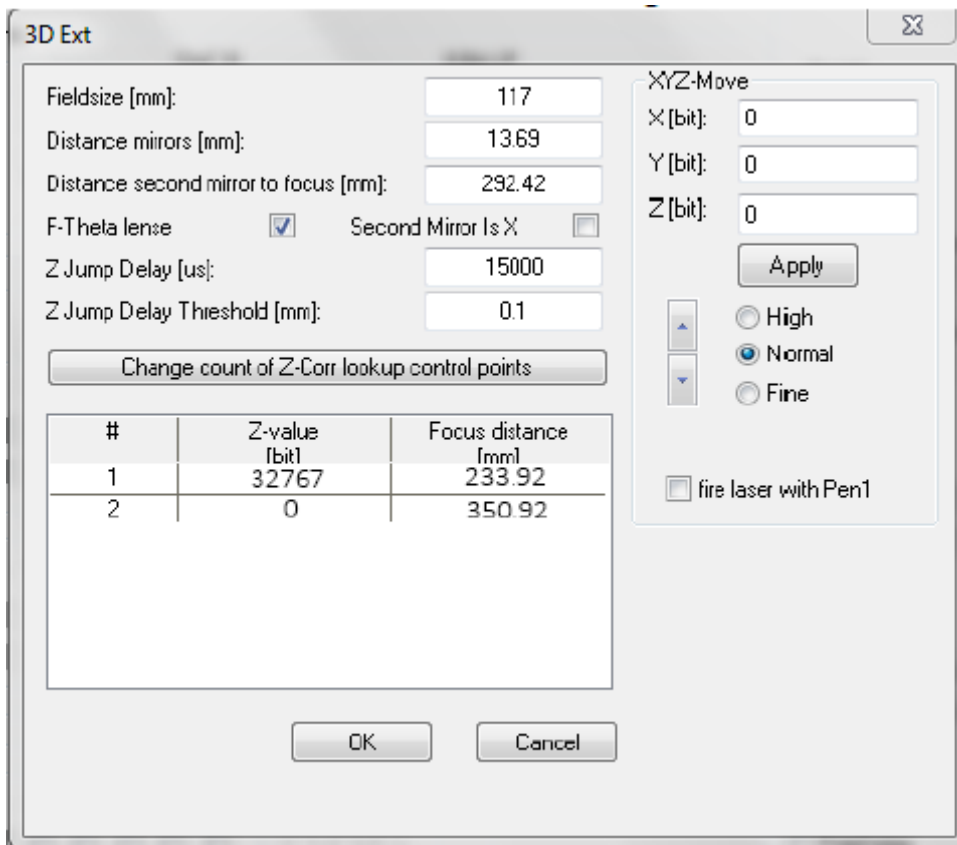
Figure 13: Comparison of marking quality with and without the STOT-EL-10-42-OF in the beam path. Under the microscope (8x mag.), no difference between the two situations.

Appendix: How to perform z-calibration with STOT-EL-10-42-OF in SAMLight

The following procedure describes one possible way to calibrate the z-position of the marking laser spot against the control voltage. The method has been successfully tested in a standard marking system described in this application note. The obtained precision is 500 μm . For higher precision, a beam profile measurement is recommended. The marking software SAMLight (SCAPS) allows for easy integration of the z-calibration via a look-up table. The coordinate system is defined as:



1. It is assumed that the distance D from second mirror to the working plane is already known (in the exemplary system, $D = 292.42 \text{ mm}$). Before integrating the STOT-EL-10-42-OF, this has to be measured precisely, e.g. with the help of a mechanical z-stage.
2. As a first step, a temporary z-correction look-up table has to be created. The measurements done with this table will allow for deducing the final z-correction table.



3D Ext

Fieldsize [mm]: 117

Distance mirrors [mm]: 13.69

Distance second mirror to focus [mm]: 292.42

F-Theta lense Second Mirror Is X

Z Jump Delay [us]: 15000

Z Jump Delay Threshold [mm]: 0.1

Change count of Z-Corr lookup control points

| # | Z-value [bit] | Focus distance [mm] |
|---|---------------|---------------------|
| 1 | 32767 | 233.92 |
| 2 | 0 | 350.92 |

XYZ-Move

X [bit]: 0

Y [bit]: 0

Z [bit]: 0

Apply

High

Normal

Fine

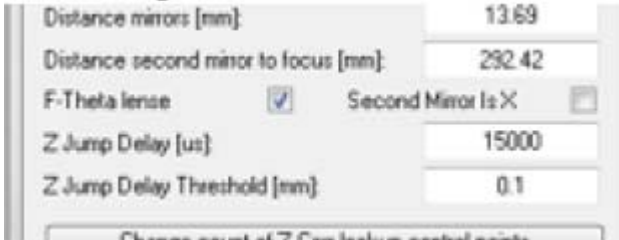
fire laser with Pen1

OK Cancel

The table is defined only by the two DAC end points DAC1 = 32767 and DAC2 = 0, which correspond to 0 and 5V respectively. This is the maximum allowed range of the lens' control voltage. The corresponding distances (mm) are calculated as seen in the table below:

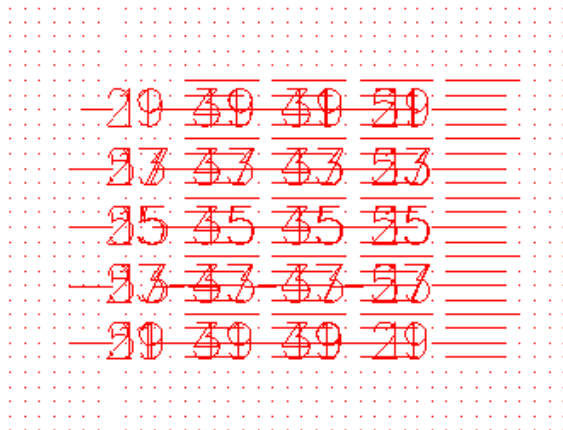
| | | |
|------------------|-------|---|
| DAC ₁ | 32767 | $D - (x,y\text{-working area} / 2) = D_1$ |
| DAC ₂ | 0 | $D + (x,y\text{-working area} / 2) = D_2$ |

3. When using an f-theta lens, the corresponding check box in SAMLIGHT has to be enabled.

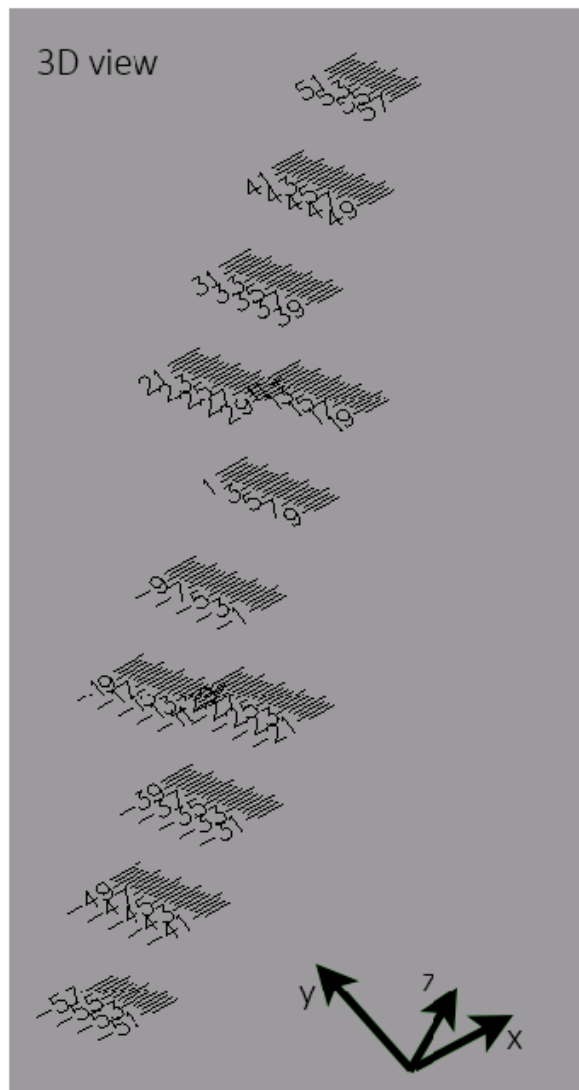


4. Load the pre-defined marking job file "Find_DAC_Values.sjf" in SAMLIGHT.

Top view



3D view



This job file serves as a vertical "ruler". It consists of lines ranging from -57...+57 mm in z-direction. The lines have 0.5 mm spacing. If your x,y-working area is smaller than this range, you have to delete a few lines in the job file such that the z-range < x,y-working area. Otherwise the error message "Galvo out of range" will appear when clicking "start mark".

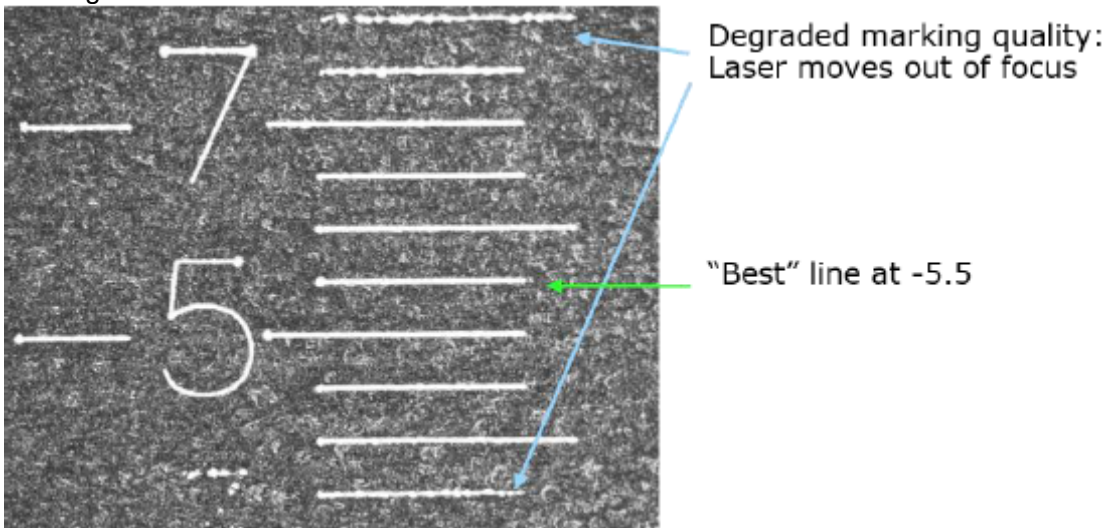
5. Next, define the number of z-values of the final z-correction table in a separate spread sheet. The points have to be within the maximum physical z-tuning range (e.g. -45...+45 mm). For example:

| z-value (mm) |
|--------------|
| -38.7 |
| -17.5 |
| 0 |
| 29.8 |
| 42.6 |

6. Position a marking sample (e.g. anodized aluminum plate) at the first point of the final z-correction table (e.g. 39.82 mm in this example). According to the definition of the coordinate system, a negative z-value (mm) means below the zero plane and a positive value above the zero plane. This is consistent with the definition of the coordinate system in SAMLight. Start marking the job file.

7. Change the z-position of the marking sample to the next point of the final z-correction table and mark the job file again. Repeat this procedure for all z-values.

8. Extract the marked z-position values F_z from the marking sample. To do so it is helpful to analyze the samples under a standard microscope (e.g. 8x magnification). This increases the precision when locating the "best" line that was in focus.



9. After this analysis, your z-correction table might look like shown below. At z-value = 0 mm, the marked value on the sample is not necessarily zero due to a possible offset. The calibration will take this offset automatically into account.

| z-value (mm) | F_z (marked value on sample) |
|--------------|--------------------------------|
| -38.7 | -34 |
| -17.5 | -17.5 |
| 0 | -1 |
| 29.8 | 34 |
| 42.6 | 48.5 |

10. Next, calculate the distances $D_z = D - F_z$ with $D = 292.42$ mm in this example. As a next step, in order to establish the linear relation between the DAC values and the values D_z we have to calculate

$$DAC_z = a \cdot D_z + b$$

with the coefficients (from step 2.)

$$a = \frac{DAC_2 - DAC_1}{D_2 - D_1}, \quad b = \frac{D_2 \cdot DAC_1 - D_1 \cdot DAC_2}{D_2 - D_1}$$

Now, the table looks like below

| z-value (mm) | F_z (marked value on sample) | D_z | DAC_z |
|--------------|------------------------------|--------|-------|
| -38.7 | -34 | 326.42 | 6861 |
| -17.5 | -17.5 | 309.92 | 11482 |
| 0 | -1 | 293.42 | 16103 |
| 29.8 | 34 | 258.42 | 25906 |
| 42.6 | 48.5 | 243.92 | 29966 |

11. As a final step, one has to calculate D – (z-value). D is the distance from 2nd mirror to working area. The final look-up table implemented in SAMLight, highlighted in red, looks like:

| z-value (mm) | F_z (marked value on sample) | D_z | DAC_z | z-value absolute (mm) |
|--------------|------------------------------|--------|-------|-----------------------|
| -38.7 | -34 | 326.42 | 6861 | 331.12 |
| -17.5 | -17.5 | 309.92 | 11482 | 309.92 |
| 0 | -1 | 293.42 | 16103 | 292.42 |
| 29.8 | 34 | 258.42 | 25906 | 262.62 |
| 42.6 | 48.5 | 243.92 | 29966 | 249.82 |

The two red columns are used in SAMLight as the final z-calibration look-up table. Note that in SAMLight, the “Focus distance (mm)” has to be entered in ascending order:

| Z-value (bit) | Focus distance (mm) |
|---------------|---------------------|
| 29966 | 249.82 |
| 25906 | 262.62 |
| 16103 | 292.42 |
| 11482 | 309.92 |
| 6861 | 331.12 |

12. Optional: one can perform a verification measurement. If the calibration is correct, one obtains the same values when repeating steps 5 to 8. The exemplary measurement shown below confirms this relation. The deviations are small and within the precision of the method described in step 8.

